Oxide-apertured microcavity single-photon-emitting diodes—simultaneous confinement of current and light

2008 J. Phys.: Condens. Matter 20 454212

(http://iopscience.iop.org/0953-8984/20/45/454212)

J. Phys.: Condens. Matter **20** (2008) 454212 (5pp) doi:10.1088/0953-8984/20/45/454212

Oxide-apertured microcavity single-photon-emitting diodes—simultaneous confinement of current and light

David J P Ellis[1], Anthony J Bennett[1], Samuel J Dewhurst[1,2], Paola Atkinson[2], Christine A Nicoll[2], David A Ritchie[2] and Andrew J Shields[1]

[1] Toshiba Research Europe Limited, 208 Cambridge Science Park, Milton Road, Cambridge CB4 0GZ, UK
[2] Cavendish Laboratory, University of Cambridge, J J Thomson Avenue, Cambridge CB3 0HE, UK

E-mail: david.ellis@crl.toshiba.co.uk

Received 6 May 2008
Published 23 October 2008
Online at stacks.iop.org/JPhysCM/20/454212

Abstract
We report on the development of a generation of microcavity single-photon sources in which an aluminium oxide aperture provides simultaneous confinement of the injected current and the optical mode. The aperture is formed by the wet oxidation of an aluminium-rich AlGaAs layer. This approach allows a high quality cavity to be successfully integrated into an electrical device, from which enhanced photon emission is observed through the Purcell effect. The resulting source demonstrated an improved photon collection efficiency and was shown to operate at repetition rates in excess of 0.5 GHz.

(Some figures in this article are in colour only in the electronic version)

1. Introduction

The continuing advancement of the digital age has produced many benefits to mankind. However, to further improve the available technologies, ever more demanding requirements are placed on each element of a particular system.

In the field of quantum information, schemes for photonic quantum computing and quantum communication fuel a continuing thirst for high efficiency sources of single and pairs of photons. Semiconductor quantum dots (QDs) are ideal candidates for use as single-photon emitters: they can confine both electrons and holes in small numbers and, when the carriers recombine, they produce a series of sharp emission features—characterized by the combination of carriers confined in the dot [1]. Furthermore, quantum dots emit antibunched photons, that is to say that the emission statistics show a reduced probability of the simultaneous emission of more than one photon from a particular state.

When embedded in GaAs, self-assembled InAs QDs may be excited optically by means of a pump laser that is focussed onto the sample or, if the quantum dots are embedded in a p–i–n diode structure, they may be electrically excited [2]. To achieve a practical source, electrical injection is particularly favourable as it eliminates the necessity for a pump laser and associated optics.

Quantum dots alone are not, however, the solution. If a quantum dot is embedded in bulk GaAs, total internal reflection at the air–GaAs interface dramatically reduces the fraction of emitted photons that can escape the crystal. If an objective lens of numerical aperture (NA) 0.5 is then used to collect the emission, it can be shown that, at most, only 0.5% of the emitted photons could be coupled into an experiment [3]. It is well known that embedding the quantum dots in a microcavity structure can increase the efficiency with which the photons are collected [4]. Furthermore coupling the QD emission to a confined cavity mode also provides a route to control the radiative dynamics of the source through the

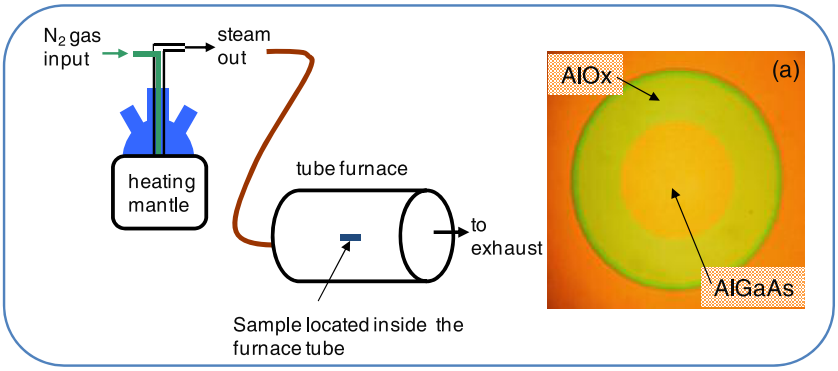

Figure 1. Schematic of a typical wet oxidation system. Photograph (a) shows an optical microscope image of a partially oxidized mesa containing a single AlGaAs oxidation layer. The colour difference between the oxidized and unoxidized regions is due to the refractive index contrast between the AlOx and AlGaAs.

Purcell effect. This is of particular importance for guaranteeing indistinguishable photons [5] and realizing high repetition rate devices.

One of the most widely studied designs has been based on pillar microcavity structures, which consist of a pair of distributed Bragg reflectors (DBRs), comprising alternating layers of AlGaAs and GaAs, surrounding a GaAs cavity spacer [6–9]. This cavity region contains the QDs. In this paper, we will describe how a wet oxidation process can be used to modify the properties of these structures by converting a layer of aluminium-rich AlGaAs into dense, stable aluminium oxide (hereafter 'AlOx').

2. Wet oxidation of AlGaAs

The wet oxidation process for aluminium gallium arsenide was discovered at the University of Illinois in the early 1990s [10] during a study of the destructive atmospheric hydrolysation process that occurs at room temperature. The researchers realized that if steam oxidation is carried out at an elevated temperature (typically around 400 °C) a different chemical reaction occurs which converts the AlGaAs into a dense, stable aluminium oxide. Steam is generated by bubbling a carrier gas, generally nitrogen, through de-ionized water held close to 100 °C. The resulting oxide is an excellent electrical insulator and has a refractive index of around 1.5. A typical oxidation system is shown schematically in figure 1.

Oxidation can proceed vertically into surface layers of AlGaAs and also laterally into buried layers through exposed sidewalls. In this way, layers of oxide can be formed within etched mesas. Furthermore, if the oxidation is terminated before the AlGaAs layer is completely oxidized, a ring of oxide may be formed within the structure. Figure 1(a) shows an optical microscope photograph of a mesa that has been etched and partially oxidized. The refractive index contrast between the AlOx and the unoxidized AlGaAs at the centre of the mesa is clearly visible as a colour change in the image. Such oxide apertures have been shown to work effectively as current apertures, allowing the electrically active area of a large structure to be reduced to micron or sub-micron length scales [11]. Recently this approach has been used to electrically isolate a single InAs quantum dot in a p–i–n diode [12].

In addition to aperture structures, buried AlGaAs layers can be completely oxidized, for example to form high reflectivity AlOx/GaAs distributed Bragg reflectors [13]. As a brief aside: in conventional GaAs/AlGaAs microcavity structures a large number of mirror periods are required to achieve high quality factor (Q) cavities, leading to structures many microns high. However, the AlOx/GaAs material combination achieves a reflectivity ∼15% higher at each interface, allowing high Q structures to be realized with far fewer mirror periods. In addition, the penetration of light into these mirrors is reduced, allowing such a cavity to confine photons within a very small volume and modifying the emission dynamics of a coupled quantum state through the Purcell effect.

3. Oxide-apertured microcavities

The pillar microcavity has been extensively studied and utilized a number of different materials systems to form the DBR layers—including GaAs/AlGaAs and GaAs/AlOx. In all cases, lateral confinement of the optical mode is produced at the air–semiconductor interface of micron-sized etched pillars. Whilst extremely high quality pillar microcavities have been fabricated using techniques such as inductively coupled plasma (ICP) etching [9], the pillar geometry has several disadvantages. Firstly, the quality factor of the confined modes falls as the pillar diameter is reduced. This is caused by the roughness of the pillar sidewalls, from which light can scatter and couple into leaky modes. Whilst these effects can be minimized through extensive process optimization, scattering is likely to persist to some degree. Secondly, the high aspect-ratio pillar is not ideally suited for integration into an electrically driven device. Maintaining a micron-sized pillar cross-section (to achieve low mode volume) whilst achieving reliable electrical contact provides a number of technological challenges.

One solution is to employ a much larger mesa and to independently realize lateral modal confinement. In the same way that the air–semiconductor interface of a pillar results

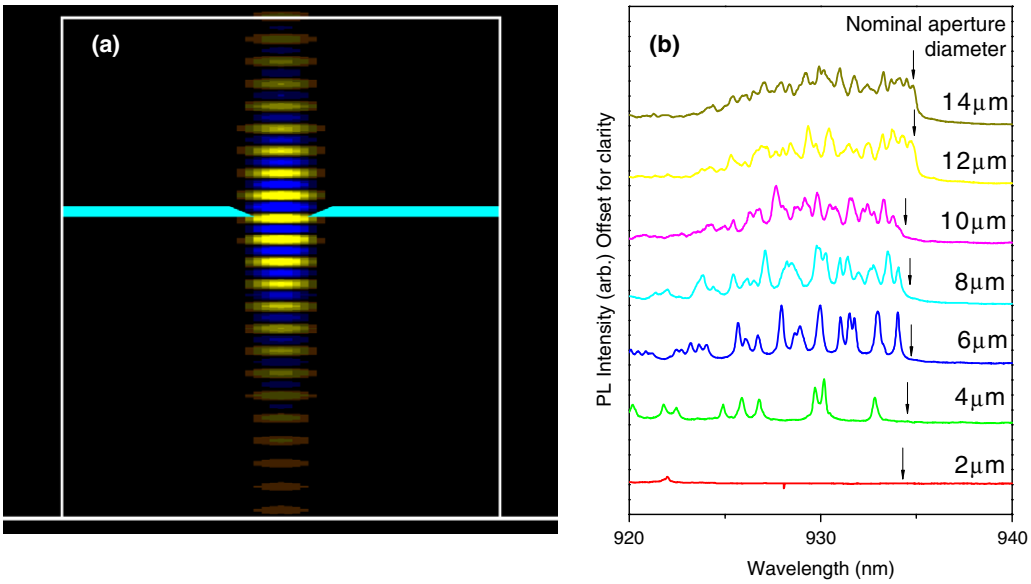

Figure 2. (a) FDTD simulation of the electric field profile of the HE_{11} mode in an oxide-confined microcavity structure. The blue lines represent the oxide aperture. (b) Evolution of cavity mode spectra from oxide-confined devices with reducing nominal aperture diameter. As the diameter falls, the modes blueshift and become separated.

in lateral confinement, similar results can be achieved by modifying the lateral effective refractive index profile of a cavity structure by adding an annulus of low refractive index AlOx. The shape and profile of the oxide aperture has been shown to have a impact on modal confinement [14–16]. Linearly tapered profiles produce in a more gradual change in effective refractive index and result in reduced scattering and higher quality structures. To this end, a tapered aperture profile has been employed in the structures discussed in this work [17].

Figure 2(a) shows the calculated profile of the HE_{11} mode in an oxide-confined microcavity consisting of 17(25) period GaAs/AlGaAs DBRs above (below) the cavity respectively. The blue layer corresponds to the oxide aperture in the structure. As expected, the aperture results in a well-confined optical mode that is well isolated from the mesa sidewalls.

The mode profile, measured in photoluminescence (PL) from a set of cavity structures is shown in figure 2(b). As the diameter of the oxide aperture is reduced, the group of optical modes observed in the planar structure breaks into a number of resonant modes. As the diameter is reduced, the modes blueshift relative to the planar cavity mode (indicated by the black arrow in each case) and the mode spacing increases. Similar characteristics are observed in conventional pillar microcavities, where the confinement is provided solely by the semiconductor–air interface of the pillar. The origin and assignment of these modes is well understood from work on circular cross-section optical fibres [18] and the longest wavelength peak is the on-axis HE_{11} mode.

The blueshift of the HE_{11} mode with reducing aperture dimension can be understood using a simple 'waves-in-a-box' model. It can be shown that the wavelength of the mode varies with aperture radius such that $\lambda(r) = \lambda_0 - C/(n_{\text{eff}}^2 r^2)$, where λ_0 is the wavelength of the planar cavity mode and C is a constant. Using the experimentally determined blueshift, this model provides a useful tool to verify the dimensions of a buried aperture layer—which cannot be directly measured using an indestructive method.

4. Oxide-apertured microcavity single-photon-emitting diodes

The integration of a high-Q cavity with an electrically driven device represents an important step forward: achieving a significant Purcell enhancement would lead to increased photon collection efficiencies and shorter state lifetimes. However, until recently all demonstrations of Purcell-enhanced QD emission had relied upon optically exciting carriers by means of a pump laser.

The addition of doping to the oxide-apertured microcavity structures discussed here allows carriers to be electrically injected into the device whilst maintaining a high quality cavity. Indeed, an enhancement in the radiative emission rate has now been demonstrated in such a structure [19]. In these circumstances, the oxide aperture assumes a dual role and simultaneously confines the current and the optical mode to the centre of mesa. In this way, a physically large (tens of microns) structure can be fabricated that has a micron-sized electrically active area and mode width. Furthermore, electroluminescence (EL) will only be observed from QDs located in the current path formed underneath the aperture.

Figure 3(a) plots the EL spectrum recorded from once such device at 48 K. At this point, an X^+ state from a quantum dot located beneath the aperture is coupled to the HE_{11} cavity mode. Emission from this state dominates the spectrum. Figure 3(b) shows the measured evolution in the radiative decay rate of this QD state as it is tuned across the cavity mode. A enhancement in the radiative decay rate was observed, corresponding to a Purcell factor of (2.49 ± 0.05). Evaluation of the efficiency with which photons can be collected from the

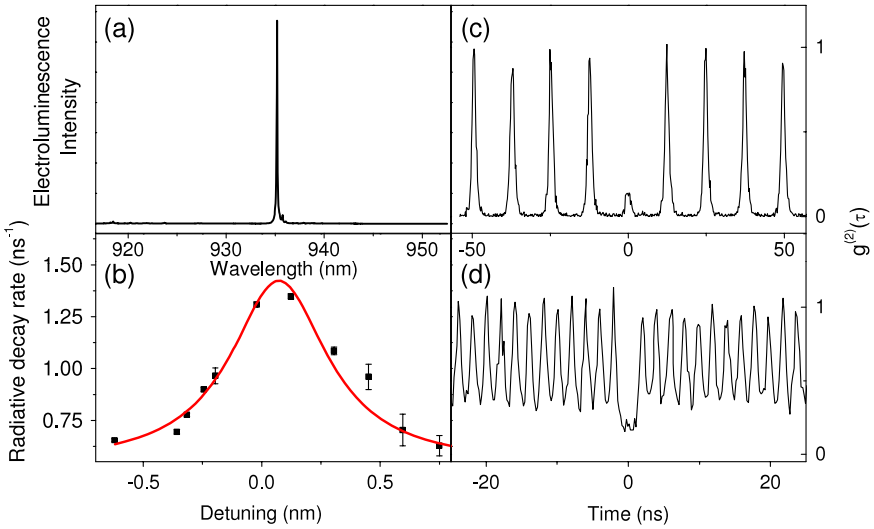

Figure 3. (a) Electroluminescence spectrum recorded from the X^+ state of a QD, coupled to the HE_{11} cavity mode at 48 K. (b) Evolution in the radiative emission rate of the X^+ state as a function of detuning from the HE_{11} mode. When on resonance, the enhancement corresponds to a Purcell factor of 2.5. ((c), (d)) Autocorrelation histograms recorded under resonance conditions. (c) Measurement performed at a repetition rate of 80 MHz with a time-averaged current of 1 nA. A strong suppression of the zero delay peak was observed, with $g^{(2)}(0) = 0.17$, confirming the emission of single photons. (d) Measurement repeated at a repetition rate of 0.5 GHz with no increase in $g^{(2)}(0)$. This demonstrates the flexibility of the electrically driven, oxide-confined single-photon-emitting diode.

device yielded a value of $14 \pm 1\%$, corresponding to a 28-fold improvement over simple structures without a cavity [2, 3, 12].

To verify that the device was producing single photons, the photon emission statistics were studied using a Hanbury-Brown and Twiss coincidence arrangement. When driven at a repetition rate of 80 MHz with a time-averaged current of 1 nA, a strong suppression of the zero-time-delay peak was observed with a measured $g^{(2)}(0)$ of 0.17 as shown in figure 3(c). This confirmed the emission of single photons from the source. As the repetition rate of the device is controlled by the driving electronics, it was straightforward to repeat the experiment at higher frequencies. Figure 3(d) shows the autocorrelation histogram recorded for a repetition rate of 0.5 GHz. The peaks in the histogram are broadened by the decay rate of the X^+ state and the finite response time of the system. Consequently adjacent peaks begin to overlap. However, we again observe a strong suppression of coincidence counts in the $\tau = 0$ peak, together with no increase in $g^{(2)}(0)$ when compared to operation at 80 MHz.

5. Conclusions

To conclude, employing oxide confinement in microcavity structures has allowed high quality electrically driven single-photon sources to be produced. The oxide aperture simultaneously confines the current path and optical mode within the structure. Purcell-enhanced emission has been realized, leading to an improved photon collection efficiency of 14% and a factor of $\sim$2.5 enhancement in the radiative emission rate. Using pulsed electrical injection, single-photon emission at repetition rates in excess of 0.5 GHz has been achieved without degradation in $g^{(2)}(0)$. Further improvements to the device could allow higher Purcell factors and repetition rates to be achieved.

Acknowledgments

The authors would like to acknowledge support from the European Commission under Integrated Project SECOQC, the Integrated Project Qubit Applications (QAP) funded by the IST directorate as contract number 015848 and Framework Package 6 Network of Excellence SANDiE. CAN would also like to acknowledge support from the EPSRC QIP IRC.

References

[1] Shields A J 2007 *Nat. Photon.* **1** 215–23
[2] Yuan Z L, Kardynal B E, Stevenson R M, Shields A J, Lobo C J, Cooper K, Beattie N S, Ritchie D A and Pepper M 2002 *Science* **295** 102
[3] Bennett A J *et al* 2006 *Phys. Status Solidi* b **243** 3730
[4] Vahala K J 2003 *Nature* **424** 839–46
[5] Santori C, Fattal D, Vučković J, Solomon G and Yamamoto Y 2002 *Nature* **419** 594
[6] Moreau E, Robert I, Gérard J, Abram I, Manin L and Thierry-Mieg V 2001 *Appl. Phys. Lett.* **79** 2865
[7] Solomon G S, Pelton M and Yamamoto Y 2001 *Phys. Rev. Lett.* **86** 3903
[8] Reithmaier J P, Sek G, Löffler A, Hofmann C, Kuhn S, Reitzenstein S, Keldysh L, Kulakovskii V, Reinecke T L and Forchel A 2004 *Nature* **432** 197
[9] Reitzenstein S, Hofmann C, Gorbunov A, Strauß M, Kwon S H, Schneider C, Löffler A, Höfling S, Kamp M and Forchel A 2007 *Appl. Phys. Lett.* **90** 251109
[10] Dallesasse J M, Holonyak N Jr, Sugg A R, Richard T A and El-Zein N 1990 *Appl. Phys. Lett.* **57** 2844
[11] Zinoni C, Alloing B, Paranthoën C and Fiore A 2004 *Appl. Phys. Lett.* **85** 217
[12] Ellis D J P, Bennett A J, Shields A J, Atkinson P and Ritchie D A 2006 *Appl. Phys. Lett.* **88** 133509
[13] Bennett A J, Ellis D J P, Shields A J, Atkinson P, Farrer I and Ritchie D A 2007 *Appl. Phys. Lett.* **90** 191911

[14] Monat C, Blandine A, Zinoni C, Li L H and Fiore A 2006 *Nano Lett.* **6** 1464
[15] Huffaker D L, Deppe D G and Rogers T J 1994 *Appl. Phys. Lett.* **65** 1611
[16] Hegblom E R, Thibeault B J, Naone R L and Coldren L A 1997 *Electron. Lett.* **33** 869
[17] Ellis D J P, Bennett A J, Shields A J, Atkinson P and Ritchie D A 2007 *Appl. Phys. Lett.* **90** 233514
[18] Yariv A 1997 *Optical Electronics in Modern Communications* (Oxford: Oxford University Press)
[19] Ellis D J P, Bennett A J, Dewhurst S J, Nicoll C A, Ritchie D A and Shields A J 2008 *New J. Phys.* **10** 043035